International Journal of Internet, Broadcasting and Communication Vol.9 No.1 64-71 (2017)
https://doi.org/10.7236/IJIBC.2017.9.1.64

IJIBC 17-1-10

Inductive Sensor and Target Board Design for Accurate Rotation Angle Detection

Jae-Jeong Hwang[1*] and Joon Moon[2]

[1]*Dept. IT Convergence & Commun. Eng., Kunsan National University, Korea*
[2]*JF Systems Ltd., Korea*
E-mail: [*]hwang@kunsan.ac.kr, jmoonkor@gmail.com

Abstract

In the commercial building such as huge enterprise building, more accurate operation of the center-controlled roller blind. We design, in this work, the target disc that its shape is nonlinearly changing and the sensor coils that are differentially arranged. The performance shows less than 1% accuracy when it is implemented in the roller blind.

Keywords: *Inductive Sensing, Eddy current, Non-destructive Testing, Sensor board, Target board, Roller Blind, Rotation Angle Detection*

1. Introduction

For many years inductive sensors have been broadly used for many different tasks, for example as distance and approximation sensors in measurement of linear and rotational movement. When a metal on the target is place in close proximity to the sensor coil, the induced current produces a counter field that reduces the effective inductance of the sensor coil, thus changing the resonant frequency and electric voltage [1]. Using the phenomena, we can measure distance between two conductors with no contact [2]. In the presence of inductive field changes, current in the target varies, so called eddy current, and these field perturbations are then processed to infer physical or geometrical characteristics [3]. The eddy current testing (ECT) has been widely used for non-destructive testing and material defectoscope [4].

In the application of roller blind, moving up and down, distance between two conductors is fixed and induced eddy current does not change. Thus, we need to introduce variable shape of the target that is changed by rotation of the sensor coil. The amount of the coil-target overlap changes as the target rotates. Overlapped area can be used to measure rotational angle. To accomplish the task, we design the target disc and corresponding sensor coil.

Texas Instruments have developed multi-channel inductance to digital converter chipset [5][6] to be used

Manuscript Received: Jan. 20, 2017 / Revised: Jan. 31, 2017 / Accepted: Feb. 6, 2017
Corresponding Author: hwang@kunsan.ac.kr
Tel:+82-63-469-4855, Fax: +82-63-466-2086
Dept. IT Convergence & Commun. Eng., Kunsan National University

for linear and rotational encoders. However, in order to correctly design and implement the target and sensor board, calculation of overlapping areas should be solved in an analytical manner. In this paper, we solved analytic properties of the overlapping phenomena in the target and sensor board. As results, we design and implement the two boards for application to commercial roller blind.

2. Modeling for inductive sensing

The principle of inductive sensing is based on the variation of inductance when a conductive material, such as a metal object, is placed in a magnetic field of the sensor coil. Figure 1 shows an electrical model for inductive sensor and target material [5]. The eddy current induced on the target is a function of distance, size, and composition of the conductor. The voltage across the sensor coil is represented by

$$V_P = L_{SS}\frac{dI_1}{dt} - M\frac{dI_2}{dt} \tag{1}$$

where L_{SS} and M denote inductance in the sensor coil and mutual inductance by interacting with the target. That is, inductance L_{SS} is affected by target inductance L_{ST}.

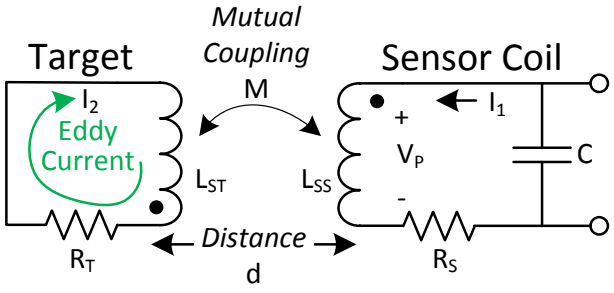

Figure 1. Electrical model for inductive sensor and target.

In Figure 1, the mutual inductance M increases, as the sensor coil come closer to the target, and the magnetic field strength at the target increases, resulting in increased eddy current. Thus, the total voltage induced on sensor coil decreases. When the distance between the target and sensor increases, the total voltage also increases. By this principle, we can measure the distance or the existence of object, operating in vicinity of the target.

In case of fixed distance, it is possible to measure the eddy current, assuming that a part of sensor coil is corresponding with the target, while the other part is out of the magnetic field. The total voltage varies with the corresponding overlapping area between the target and sensor coil. The more area overlapped, the less voltage V_P is achieved. This case is called lateral proximity configuration [6] which is being considering in our work. Problem is that we need to calculate the overlapped area by the analytic method discussed in following section.

3. Target board and sensor coil design

Although the eddy current is a function of distance between sensor and target, we assume that the distance is fixed but area of conductor may change depending on the rotation angle, since the sensor is located on the roller blind bracket [7]. Figure 2 depicts the target and sensor coil that are overlapped when

rotating. Though the thickness between two circles is linearly variable on the rotation angle, the overlapped area is nonlinearly changing.

Target board is composed of three circles C_1, C_2, and C_3, centered on (0, 0), (-0.25, 0), and (0.25, 0), respectively. Sensor coil is rotated on target with overlapping area, centered around the circle C_1, which is calculated by polar coordinate as

$$\begin{pmatrix} x_{C4} = r_{C1}\cos\theta \\ y_{C4} = r_{C1}\sin\theta \end{pmatrix}, \quad 0 \le \theta \le 360 \tag{3}$$

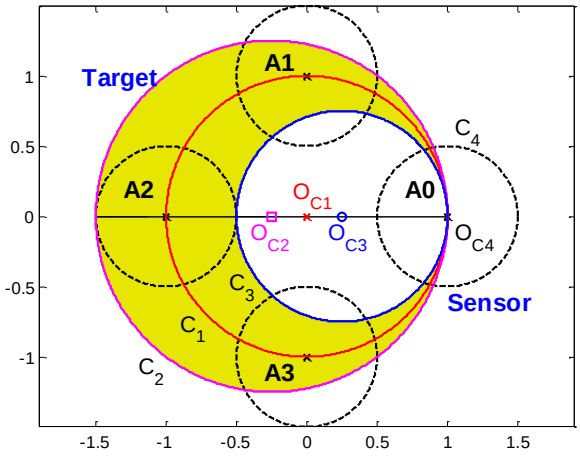

Figure 2. Design of target board and overlapping four sensor coils.

a) Intersection of two circles

There are two cases, when the two circles have intersection: acute angle case and obtuse angle case as shown in Figure 3. In general case, such as a small portion of circle are intersected, angle from the center of circle is acute as shown in Figure 3 left. First, we compute distance between the two circles by

$$R = \sqrt{(x2-x1)^2 + (y2-y1)^2} \tag{4}$$

The two intersection coordinates (x_{i1}, y_{i1}) and (x_{i2}, y_{i2}) are calculated as

$$\begin{aligned} x_{i1} &= a(x1+x2) + b(x2-x1) + c(y2-y1) \\ y_{i1} &= a(y1+y2) + b(y2-y1) + c(x1-x2) \\ x_{i2} &= a(x1+x2) + b(x2-x1) - c(y2-y1) \\ y_{i2} &= a(y1+y2) + b(y2-y1) - c(x1-x2) \end{aligned} \tag{5}$$

where *a*, *b*, and *c* are given by

$$\begin{aligned} a &= 1/2 \\ b &= (r1^2 - r2^2)/(2R^2) \\ c &= 1/2\sqrt{2(r1^2+r2^2)/R^2 - (r1^2-r2^2)^2/R^4 - 1} \end{aligned} .$$

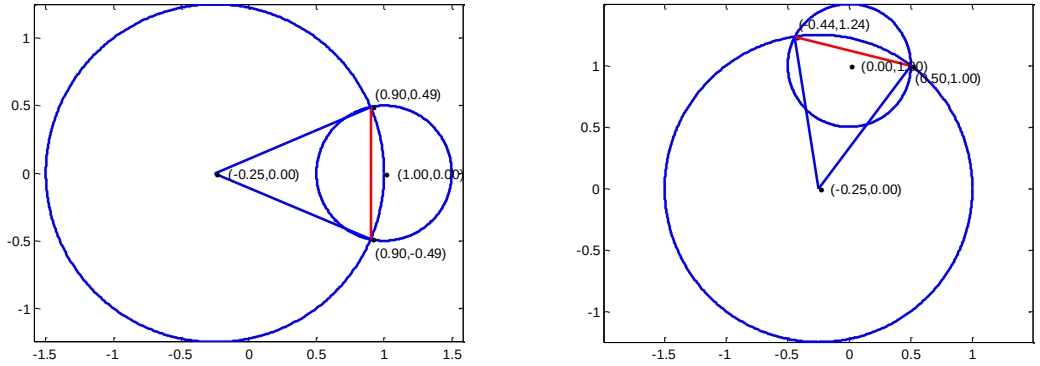

Figure 3. Intersection of two circles in acute angle (left, $\theta = 0$) and obtuse angle (right, $\theta = \pi / 2$).

Overlapped area is calculated from cones of two circles, taking regard of triangle area that can be obtained by using Heron's rule.

$$A_{tri} = \sqrt{s(s - R_{seg}) \cdot (s - r2)^2}, \quad s = (R_{seg} + 2 \cdot r2) / 2 \tag{6}$$

where R_{seg} and $r2$ denote length of intersection coordinates and radius of circle C_2. The two arc areas are added to get total intersection area.

b) Line equation thru two points

Given two points (x_1, y_1) and (x_2, y_2), linear equation is represented by linear algebra

$$y = \frac{y_2 - y_1}{x_2 - x_1}(x - x_1) + y_1. \tag{7}$$

It can be expressed by general equation as

$$Ax + By = c, \quad \begin{cases} A = y_2 - y_1 \\ B = x_1 - x_2 \\ C = A \cdot x_1 - B \cdot y_1 \end{cases} \tag{8}$$

c) Intersection of two lines

Given two lines, their linear equations are given by using Eq. (8)

$$\begin{aligned} A_1 x + B_1 y &= C_1 \\ A_2 x + B_2 y &= C_2 \end{aligned} \tag{9}$$

Intersection point between two lines is calculated by linear operation of Eq. (9) and its coordinates are given by

$$x = \frac{B_2 C_1 - B_1 C_2}{A_1 B_2 - A_2 B_1} \quad \frac{B_2 C_1 \quad B_1}{\Delta}$$
$$y = \frac{A_1 C_2 - A_2 C_1}{A_1 B_2 - A_2 B_1} \quad \frac{A_1 C_2 \quad A_2}{\Delta} \tag{10}$$

where Δ denotes determinant. The intersection point is used to determine acute or obtuse angle discussed below.

d) Acute or obtuse angle decision

Two cases for deciding intersection area are taking into consideration. The angle from the origin of circle C_4 is acute, if the length from the origin of circle C_2 to the intersection point in Eq. (10) is less than that from C_2 to C_4. This is normal case and two intersection areas are just added.

$$A = A2 + A4 \tag{11}$$

However if it is obtuse, we apply negative operation as

$$A4 = \pi r_4^2 - (A_\theta - A_{\Delta i}) \tag{12}$$

where A_θ denotes area on angle θ.

e) Overlapping areas between target and sensor board

Target and sensor board are contactless and cooperating by induction field that vary with overlapping areas. The precision of rotation angle decision is dependent on calculation of overlapping areas when the sensor coil is rotating around the target. Eqs. (11) and (12) result in exact calculation of overlapping areas as depicted in Figure 4. Comparing with linear line, drawn in red, the overlapping areas are nonlinearly varying: smaller than normal up to $\theta = 72^\circ$ and larger than normal in the range of $72^\circ \le \theta \le 180^\circ$. The result of analytical solution is used to decide correct angle decision.

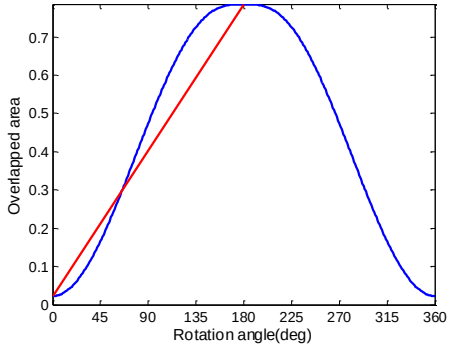

Figure 4. Intersection areas of the proposed target and sensor.

3. Rotation angle detection for roller blind

Sensor coil sets A and B are placed 90 degrees from each other, enabling the set A referred to as in-phase cosine shape and the set B referred to as quadrature sine shape as shown in Figure 5 (a). Data from each set

is derived by differential operation as

$$\begin{aligned} D_A &= D_{A+} - D_{A-} = \eta_A \cos\theta \\ D_B &= D_{B+} - D_{B-} = \eta_B \sin\theta \end{aligned} \tag{13}$$

Note that at position 0 degree, D_A becomes maximum and D_B becomes minimum. The sensitivity factor η_x equals 1, if the condition is ideal. Differential operation of A forms cosine shape, while that of B forms sine shape as shown in Figure 5 (b). They should be stretched to normal sinusoidal function as shown in Figure 5 (c).

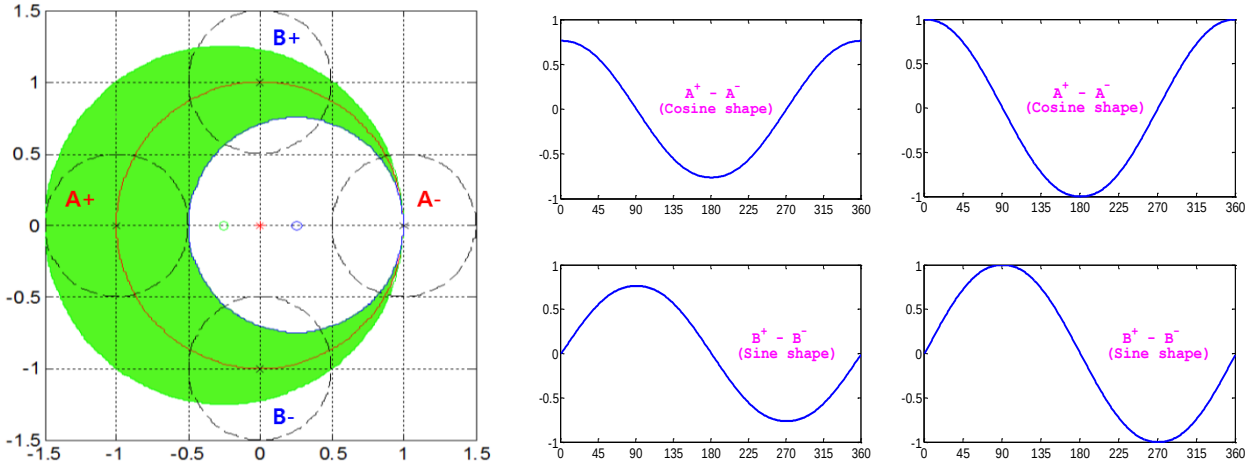

(a) (b) (c)

Figure 5. Design of target board and overlapping four sensor coils. (a) four-channel differential operation, (b) cosine and sine shape areas, and (c) stretched areas.

D_A and D_B in Eq. (2) are used to calculate the rotation angle, which is given by

$$\theta = \begin{cases} \arctan\left(\dfrac{D_B}{D_A}\right), & \text{if } D_A \geq 0 \text{ and } D_B \geq 0 \\ \arctan\left(\dfrac{D_B}{D_A}\right) + 180^\circ, & \text{if } D_A < 0 \\ \arctan\left(\dfrac{D_B}{D_A}\right) + 360^\circ, & \text{if } D_A \geq 0 \text{ and } D_B < 0 \end{cases} \tag{14}$$

4. Implementation of target and sensor board

We have implemented the target and sensor coils as shown in Figure **6. Assembled sensor coils (left) and target board(right).**6, including sensor coil antenna, microcontroller unit, oscillator, USB connector, LED indicator, and processing chipset from TI [5][6]. Target board is being rotated around sensor coils installed at the corner of the roller blind motor.

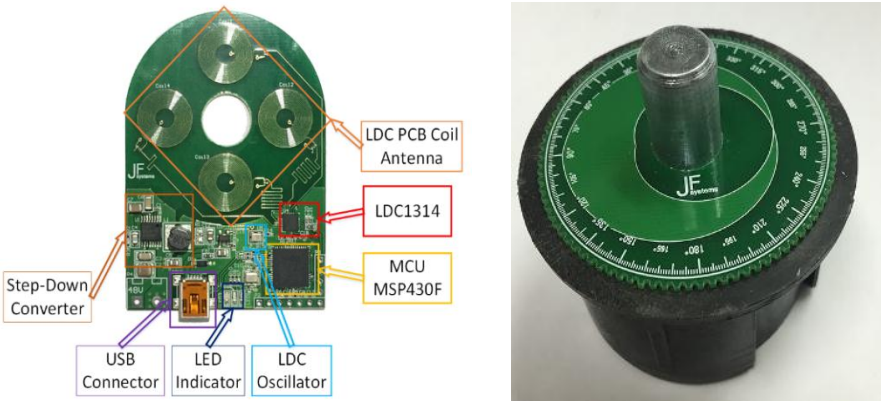

Figure 6. Assembled sensor coils (left) and target board(right).

Table 1 shows the result of accuracy of the roller blind set in terms of activation length and errors. When 30cm motion, maximum error of 2.4mm (around 0.8%) is resulted, that means highly accurate system for controlling of commercial roller blind.

Table 1. Accuracy of the proposed roller blind system.

Movement (cm)	Max. error (cm)	Error rate (%)
25	**0.146**	0.584
30	**0.24**	0.8
35	**0.197**	0.563

5. Conclusion

We design the target disc that its shape is nonlinearly changing and the sensor coils that are differentially arranged. The performance shows less than 1% accuracy when it is implemented in the roller blind. It is useful for controlling roller blind installed in large commercial building. The problem that uneven stopping in the middle of group of roller blinds due to the magnetic turbulence.

References

[1] H. Ewald and H. Krueger, "Inductive sensors and their application in metal detection," *1st Int. Conf. on Sensing Technol.*, Nov. 21-23, 2005.

[2] Cherepov, S., et al., "Optimisation of low frequency eddy current sensors using improved inductive coils and highly sensitive AMR and GMR sensor modules," *Proc. of the 13th IMEKO TC-4 International Symposium*, vol. 2, 2005.

[3] N. Benhadda, et al., "Study of the influence of conductive defect characteristics on eddy current differential probe signal," *J. of Electrical Engineering*, Nov. 2014.

[4] A. Rosell and G. Persson, "Modelling of a differential sensor in eddy current non-destructive evaluation," *Proc. of the 2011 COMSOL Conf. in Stuttgart*, 2011.

[5] Texas Instruments, *1^o Dial using the LDC1314 inductance-to-digital converter*, July 2015.

[6] Texas Instruments, *LDC1312, LDC1314 Multi-channel 12-bit inductance to digital converter (LDC) for inductive sensing*, July 2015.

[7] J. Moon and J.J. Hwang, "Inductive Sensing Based Accurate Rotation Angle Detection for Commercial Building Roller Blind," *Proc. of Int. Conf. on Innovative Appl. Res. And Edu. (ICIARE)*, vol. 3, no. 3, pp. 37-38, Dec. 2016.